Controlling Spatiotemporal Chaos with a Generalized Feedback Method *

GAO Ji-Hua(高继华)[1,2**], ZHENG Zhi-Gang(郑志刚)[3***]

[1]College of Materials, Shenzhen University, Shenzhen 518060
[2]Shenzhen Key Laboratory of Special Functional Materials, Shenzhen University, Shenzhen 518060
[3]Department of Physics, Beijing Normal University, Beijing 100875

(Received 15 September 2006)

The usual linear variable feedback control method is extended to a generalized function feedback scheme. The scheme is applied to high-dimensional spatiotemporal systems. By a combination of local generalized feedback control and the spatial coupling effect among elements, turbulent motion can be successfully eliminated.

PACS: 05. 45. Gg, 47. 27. Rc

Since the pioneering work of Ott, Grebogi, and Yorke (OGY)[1] on control of chaos and the work of Pecora and Carroll (PC)[2] on chaos synchronization in 1990, chaos control and synchronization have attracted much attention in diverse fields of nonlinear science.[3−5] In recent decades, great efforts on controlling chaos have shifted from low-dimensional systems to spatiotemporal and high-dimensional systems characterized by much larger numbers of positive Lyapunov exponents.[6−17] Spatiotemporal chaos as one type of weak turbulence may relate to the complexity in nature, for example, the turbulence in fluid dynamics. Meanwhile, spatiotemporal chaos could exhibit a large collection of rich patterns, which have great potential applications in a variety of fields, such as hydrodynamics, plasma physics, Josephson junction arrays, and chemical reactions.

To date, many control techniques in chaotic systems are included in two main methods, i.e. the nonfeedback method and the feedback scheme. For the latter, originally chaos in low-dimensional systems is controlled by applying a feedback signal input. This approach can be easily extended to the control of spatiotemporal systems with several signal injections in spatial domain, which was termed as the 'pinning' method. Recently, extensive studies on several models revealed that the existence of gradient force is of crucial importance for enhancing the control efficiency, i.e. by using only a small number of local injections (or even one) to control spatiotemporal chaos.[14−16] This finding is significant for both practical applications and theoretical interest. In practical controlling processes, one usually chooses the controller $-\varepsilon(\boldsymbol{x}-\hat{\boldsymbol{x}})$ as a negative feedback, and observes whether the forced system (the variable $\boldsymbol{x}$) can be driven to the target system ($\hat{\boldsymbol{x}}=\boldsymbol{x}$) eventually if the feedback intensity ε is properly chosen. In this feedback scheme, the system variable and the target variable have a simple linear relationship. In some cases, however, the linear feedback control cannot be effective and may even fail to achieve the target state, especially in dynamical systems with very many degrees of freedom. It is necessary to introduce other nonlinear feedback techniques to control spatiotemporal chaos. In this Letter, a generalized feedback scheme for controlling chaotic motion is proposed, which is shown to be of great feasibility and efficiency in controlling turbulence.

Consider a nonlinear dynamical system

$$\dot{\boldsymbol{x}}=\boldsymbol{R}(\boldsymbol{x},c), \tag{1}$$

where $\boldsymbol{x}$ is the state vector, and c denotes the system parameter set. Suppose that the system is chaotic for a certain choice of parameter c and assume that it has an unstable periodic solution $\hat{\boldsymbol{x}}$. The tasks of chaos control are to kill the chaotic motion in the uncontrolled system and to stabilize the system to the targeted unstable periodic orbit $\hat{\boldsymbol{x}}$. In many situations, linear variable feedback is adopted as the simplest method for controlling chaos. For example, one can simply add a variable linear feedback term on the right-hand side of Eq. (1), which is accordingly modified to

$$\dot{\boldsymbol{x}}=\boldsymbol{R}(\boldsymbol{x},c)-\varepsilon(\boldsymbol{x}-\hat{\boldsymbol{x}}). \tag{2}$$

However, in some situations, the system variable and/or the target might not be easy to be measured or collected. Therefore, the above control method is not available in some realistic applications. In the present work, we propose the generalized feedback method as a better controlling candidate. The equation of motion of the controlled system is then revised to

$$\dot{\boldsymbol{x}}=\boldsymbol{R}(\boldsymbol{x},c)-\varepsilon[\boldsymbol{G}(\boldsymbol{x})-\boldsymbol{G}(\hat{\boldsymbol{x}})], \tag{3}$$

where the feedback scheme $\boldsymbol{G}(\boldsymbol{x})$ is a function of the system state. Apparently when $\boldsymbol{G}(\boldsymbol{x})=\boldsymbol{x}$, Eq. (3) goes back to the linear feedback case of Eq. (2). Here $\boldsymbol{G}(\boldsymbol{x})$ can be chosen according to the specific situation, and thus this control scheme has more flexibility and more advantages in practical situations.

* Supported in part by the National Natural Science Foundation of China (Grants Nos. 10405018, 70571053, 70431002 and 10575010), the FANEDD (No.200120), and the TRAPOYT in Higher Education Institutions of MOE (Grant No.209).

** Email: jhgao@szu.edu.cn
*** Email: zgzheng@bnu.edu.cn

©2007 Chinese Physical Society and IOP Publishing Ltd

To analyse the controlling condition, we define an error function $\delta \boldsymbol{x} = \boldsymbol{x} - \hat{\boldsymbol{x}}$. By inserting the error function into Eq. (3), one may obtain the linearized equation

$$\delta \dot{\boldsymbol{x}} = \boldsymbol{D}\delta \boldsymbol{x}, \tag{4}$$

with $\boldsymbol{D} = \boldsymbol{dR} - \varepsilon \boldsymbol{dG}$, where $\boldsymbol{dR} = \left.\dfrac{\partial \boldsymbol{R}}{\partial \boldsymbol{x}}\right|_{\boldsymbol{x}=\hat{\boldsymbol{x}}}$ and $\boldsymbol{dG} = \left.\dfrac{\partial \boldsymbol{G}}{\partial \boldsymbol{x}}\right|_{\boldsymbol{x}=\hat{\boldsymbol{x}}}$. Without any feedback ($\varepsilon = 0$), we have at least one positive eigenvalue for the matrix $\boldsymbol{D} = \boldsymbol{dR}$ when the system is chaotic. When $\varepsilon \neq 0$, we can find the case in which all of the eigenvalues (or the real part of the complex eigenvalues) with negative $\boldsymbol{D}$ are negative for certain ε. Therefore the periodic orbit $\hat{\boldsymbol{x}}$ can be stabilized and a successful control can be achieved.

It is important to extend the above idea to the case of spatially extended systems. By considering that spatial couplings may lead to collective effect in spatiotemporal systems, one may apply the generalized feedback controller locally on some elements. The control can then be propagated through the system via couplings, and then the control is successfully achieved. Now we consider the following N coupled complex Ginzburg–Landau oscillators as our working system,[17]

$$\begin{aligned}\dot{A}_i =& A_i + r(A_{i+1} - A_{i-1}) \\ &+ (1 + \boldsymbol{i}c_1)(A_{i+1} + A_{i-1} - 2A_i) \\ &- (1 + \boldsymbol{i}c_2)|A_i|^2 A_i, \quad i = 0, 1, 2, \cdots, N-1,\end{aligned} \tag{5}$$

where A_i are complex state variables, r indicates the gradient intensity, c_1 and c_2 (both being real numbers) are system parameters. Equation (5) is a discretized (lattice) version of the one-dimensional complex Ginzburg–Landau equation, which is capable of describing the onset of a Hopf bifurcation in spatiotemporal system.[18,19] Then for the periodic boundary condition, $A_{i+N} = A_i$, Eq. (5) admits the travelling wave solutions in a very good approximation,

$$\begin{aligned}&A_i = \sqrt{1 - k^2}\exp \boldsymbol{i}(ik - \omega t), \\ &\omega = c_2 + (c_1 - c_2)k^2 - rk, \quad k = 2m\pi/N,\end{aligned} \tag{6}$$

where m is an integer. For $N \gg 1$ and $1 + c_1 c_2 < 0$, all plane wave solutions (6) have shown to be unstable, and the system exhibits turbulent motion. In this study, $c_1 = 2.1$ and $c_2 = -1.5$ are chosen to be capable of exhibiting strong defect turbulence in its asymptotic state.

Then we perform the above generalized feedback approach by driving one of the oscillators in Eq. (5). The forced oscillator can be chosen arbitrarily from any of the N oscillators due to the periodic boundary condition and the symmetry of the system. Here we simply choose the first oscillator ($i = 0$). As an example, the feedback function $\boldsymbol{G}(\boldsymbol{x})$ is set to be $\boldsymbol{G}(\boldsymbol{x}) = \dot{\boldsymbol{x}} \equiv \dfrac{dx}{dt}$, namely, only the first oscillator at the boundary is driven by the state velocity feedback signal. Thus the equation of motion of the first oscillator can be written as

$$\begin{aligned}\dot{A}_0 =& A_0 + r(A_1 - A_{N-1}) \\ &+ (1 + \boldsymbol{i}c_1)(A_1 + A_{N-1} - 2A_0) \\ &- (1 + \boldsymbol{i}c_2)|A_0|^2 A_0 - \varepsilon(\dot{A}_0 - \dot{\hat{A}}_0),\end{aligned} \tag{7}$$

and the other oscillators in Eqs. (5) remain unchanged. Here ε is the feedback intensity, and $\hat{A}_0$ is the target periodic state chosen from one of the travelling wave solutions of Eq. (6). Specifically, we choose the target state with $m = 2$ throughout the following analysis. Now our goal is to drive all N coupled complex oscillators to the periodic target state by injecting the first oscillator with the so-called velocity feedback signal. We perform numerical simulations of Eqs. (5) and (7) by using fourth-order Runge–Kutta algorithm with time steps of 2×10^{-3}, and $N = 100$.

First let us investigate the effect of the gradient force. In the absence of feedback, this bias term only influences the system frequency and does not change the stability of the system, as exemplified in Figs. 1(a) and 1(b). The similar phenomenon can be explained in the one-dimensional complex Ginzburg–Landau equation system by considering a moving coordinate frame (see Eq. (3) in Ref. [14]). With adding the velocity feedback, we systematically study the forced system at different feedback intensities and gradient forces. As an example, in Fig. 2(a), we give the evolution of error $|A_i - \hat{A}_i|$ for an arbitrarily chosen site ($i = 10$) of the coupled oscillators system for $\varepsilon = 40$ and $r = 60$. Clearly $|A_i - \hat{A}_i|$ drops to zero after a short transient period, and the system is synchronized with the target completely, implying a perfect control.

The above example presents the result of the variable velocity feedback function $\boldsymbol{G}(\boldsymbol{x}) = \dot{\boldsymbol{x}}$. In fact, other forms of feedback function $\boldsymbol{G}(\boldsymbol{x})$ with successful control have also been detected and achieved. For example, successful control can be implemented by using a sinusoidal function $\boldsymbol{G}(\boldsymbol{x}) = \sin \boldsymbol{x}$ for $\varepsilon = 100$ and $r = 80$ (shown in Fig. 2(b)), the exponential function $\boldsymbol{G}(\boldsymbol{x}) = e^{\boldsymbol{x}}$ for $\varepsilon = 100$ and $r = 60$ (shown in Fig. 2(c)), and a polynomial function $\boldsymbol{G}(\boldsymbol{x}) = 3\boldsymbol{x} + \boldsymbol{x}^3$ for $\varepsilon = 50$ and $r = 40$ (see Fig. 2(d)). Other more function forms with similar behaviour have also been tested and will not be presented here. From the above simulations, by comparing the efficiency by using controlling functions given in Figs. 2(b), 2(c), and 2(d) with the results shown in Fig. 2(a), the variable velocity feedback seems to be more efficient: $|A_i - \hat{A}_i|$ drops to a small number at a very short time, $t \approx 8$. However, the extensions of all the following conclusions drawn from $\boldsymbol{G}(\boldsymbol{x}) = \dot{\boldsymbol{x}}$ to other feedback function $\boldsymbol{G}(\boldsymbol{x})$ are straightforward.

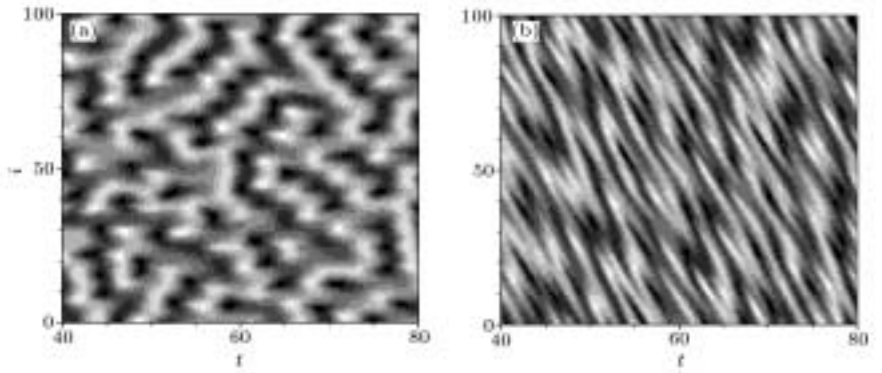

Fig. 1. Evolution of real part of system variable with different gradient forces: (a) $r = 0$ and (b) $r = 5$.

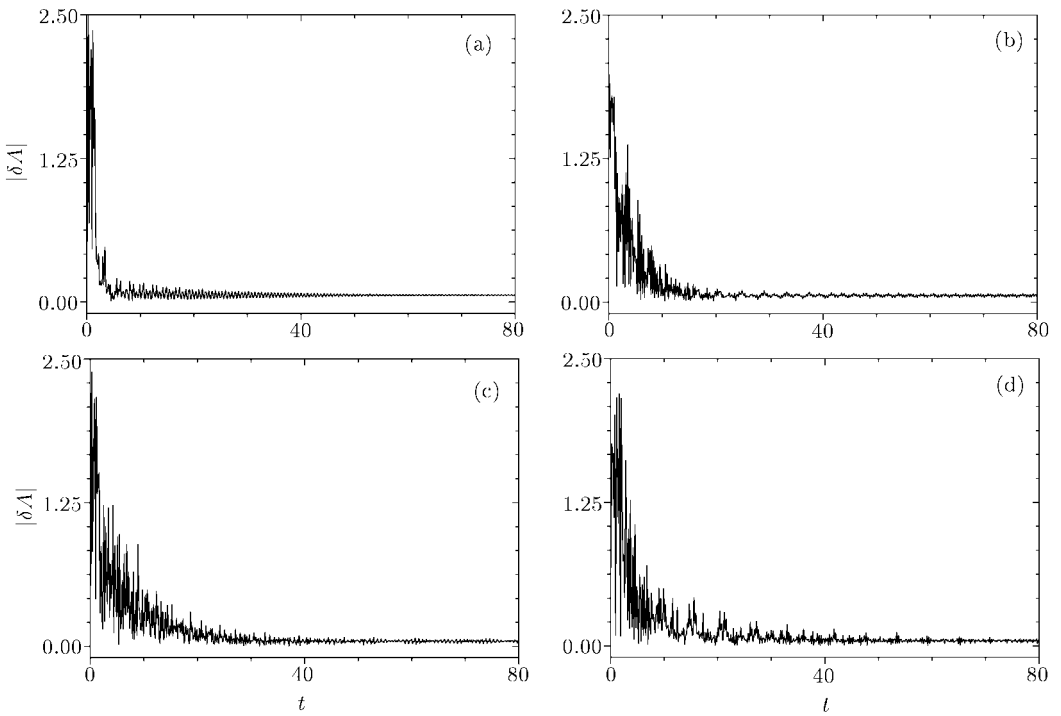

Fig. 2. $|A_i - \hat{A}_i|$ versus t for different feedback functions at $i = 10$: (a) $\boldsymbol{G}(\boldsymbol{x}) = \dot{\boldsymbol{x}}$, $\varepsilon = 40$, $r = 60$, (b) $\boldsymbol{G}(\boldsymbol{x}) = \sin \boldsymbol{x}$, $\varepsilon = 100$, $r = 80$ (c) $\boldsymbol{G}(\boldsymbol{x}) = e^x$, $\varepsilon = 100$, $r = 60$, and (d) $\boldsymbol{G}(\boldsymbol{x}) = 3\boldsymbol{x} + \boldsymbol{x}^3$, $\varepsilon = 50$, $r = 40$.

In order to obtain a whole picture for the controllability for different parameters in this velocity feedback approach, we define

$$P \equiv P(\varepsilon, r) = \lim_{T\to\infty} \frac{1}{T} \int_0^T \frac{1}{N} \sum_i |A_i - \hat{A}_i| dt \quad (8)$$

as the difference between the driving system and the target over both long-time average and ensemble average to characterize the degree of synchronization. If P drops to zero (or near zero in simulations), we achieve successful control. In contrast, for large value of P, control fails to be achieved. For a fixed feedback intensity ε, for instance, $\varepsilon = 35$, we calculate the relation between P and r as shown in Fig. 3(a). When $r > r_c \approx 55$, P drops to zero and chaos control is achieved. It is also interesting to explore the transient dynamics. Significantly we find that the system transits from the uncontrollable parameter regime to the controllable parameter regime via a quasi-periodic route. At $r = 9$ (far below r_c), the chaotic behaviour can be observed, as shown in Fig. 3(b). As the gradient force is increased to a value close to r_c, e.g. $r = 45$, we can find a torus with the quasi-periodic motion (Fig. 3(c)). At $r = 60 > r_c$, the error between the system and target is completely eliminated and we can obtain a fair periodic trajectory (the target state) (Fig. 3(d)). Therefore it is found that the gradient force plays a key role in our scheme, and sufficiently large bias flow will lead good control. An interesting feature of the controlling procedure is that a double quasi-periodic region exists in the parameter space. In Fig. 4, the real part of state versus time is plotted for different gradient forces: (a) $r = 19.1$, (b) $r = 19.2$, and (c) $r = 19.3$. Figure 4(d) is the partial meticu-

lous structure similar to Fig. 3(a). In the figure, there are two quasi-periodic states that are characterized by different P. Depending on the initial conditions and parameters, the system can evolve into one of them. In this region, the state of system may be called the alternative quasi-periodic state.

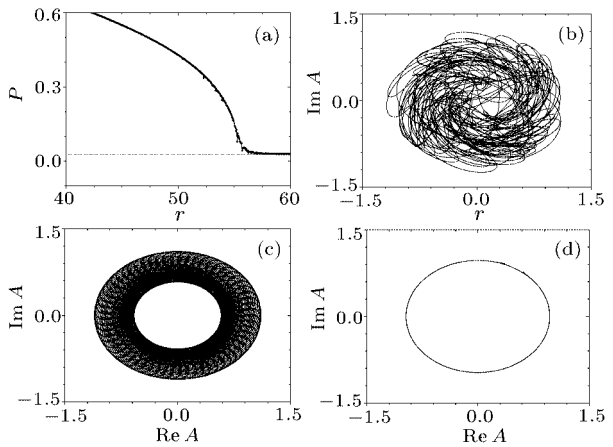

Fig. 3. System state versus different gradient force for $\varepsilon = 35$: (a) P versus r, and the phase diagrams for (b) $r = 9$, (c) $r = 45$ and (d) $r = 60$.

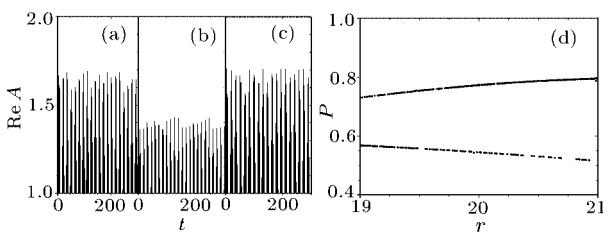

Fig. 4. Real part of state versus time: (a) $r = 19.1$, (b) $r = 19.2$, and (c) $r = 19.3$, and the corresponding structure, (d) P versus r.

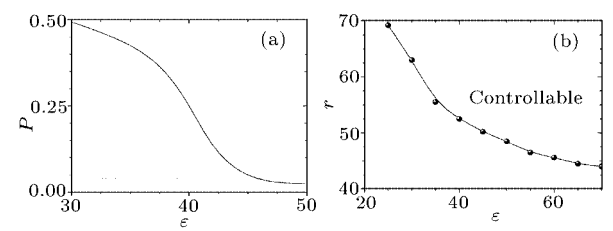

Fig. 5. Difference function versus controlling intensity for $r = 40$: (a) P versus ε, (b) controllable region in the $\varepsilon - r$ plane.

In Fig. 5(a) we plot P for the different ε and the fixed gradient strength for $r = 50$. Chaotic system can be controlled when $\varepsilon > \varepsilon_c \approx 45.1$ if we set a critical number $P = 0.04$ as our controllable condition. In Fig. 5(b), a phase diagram for the controllable regime in $\varepsilon - r$ plane is plotted. Both sufficiently large diffusive and gradient couplings can warrant the successful control.

In conclusion, we have extended the usual linear variable feedback control method to a generalized function feedback scheme. As an example, we mainly present the numerical simulation results in the variable velocity feedback approach. Other generalized feedbacks including sinusoidal, exponential, and polynomial functions are also studied. Actually, the idea of the generalized feedback method has originally been pointed out by some other researchers in the studies of low-dimensional chaos control, and carried out in a chaotic electronic circuit of the LC oscillator experiment.[20] The main contribution of the present work is to apply this scheme to high-dimensional spatiotemporal systems. On the other hand, the gradient force, as a spatial coupling effect, is common in nature: it appears in hydrodynamic flows in sloping channels, in plasma systems with electromagnetic fields, and so on.[14] By a combination of local generalized feedback control and the couplings among elements, turbulent motion can be successfully eliminated. We introduce the coupled complex Ginzburg–Landau oscillator system as our working model. The discussions can be naturally extended to other spatiotemporal systems. An interesting question how to select one proper function in our generalized feedback method with much higher efficiency is under investigation.

References

[1] Ott E, Grebogi C and York J 1990 *Phys. Rev. Lett.* **64** 1196
[2] Pecora L and Carroll T 1990 *Phys. Rev. Lett.* **64** 821
[3] Pyragas K 1992 *Phys. Lett.* A **170** 421
[4] Shinbrot T, Grebogi C, Ott E et al 1993 *Nature* **363** 411
[5] Zheng Z G, Hu G and Hu B B 2001 *Chin. Phys. Lett.* **18** 874
[6] Hu G and Qu Z L 1994 *Phys. Rev. Lett.* **72** 68
[7] Kocarev L, Parlitz U, Stojanovski T et al 1997 *Phys. Rev.* E **56** 1238
[8] Zhang X and Shen K 2001 *Phys. Rev.* E **63** 046212
[9] Xiao J H, Hu G and Hu B B 2004 *Chin. Phys. Lett.* **21** 1224
[10] Alonso S, Sagues F and Mikhailov A S 2003 *Science* **299** 1722
[11] Zhang H, Cao Z J, Wu N J et al 2005 *Phys. Rev. Lett.* **94** 188301
[12] Jiang M X, Wang X N, Ouyang Q et al 2004 *Phys. Rev.* E **69** 056202
[13] Wang X N, Lu Y, Jiang M X et al 2004 *Phys. Rev.* E **69** 056223
[14] Xiao J H, Hu G, Yang J Z et al 1998 *Phys. Rev. Lett.* **81** 5552
[15] Hu G, Xiao J H, Gao J H et al 2000 *Phys. Rev.* E **62** R3043
[16] Tang G N and Hu G 2006 *Chin. Phys. Lett.* **23** 1523
[17] Gao J H, Wang X G, Hu G et al 2001 *Phys. Lett.* A **283** 342
[18] Janiaud B, Pumir A, Bensimon D et al 1992 *Physica* D **55** 269
[19] Cross M and Hohenberg P 1993 *Rev. Mod. Phys.* **65** 851
[20] Guan S G, Li K and Lai C H 2006 *Chaos* **16** 023107